Reference ballistic chronograph

Nicholas G. Paulter, Jr.
Donald R. Larson
National Institute of Standards and Technology
Office of Law Enforcement Standards
Mailstop 8102
100 Bureau Drive
Gaithersburg, Maryland 20899-8102
E-mail: donald.larson@nist.gov

Abstract. A ballistic chronograph with an expanded uncertainty of less than ±0.2 m/s has been designed, constructed, and tested. Because of this low uncertainty, this chronograph can be used as a reference to calibrate and/or characterize the performance of commercially available chronographs.
[DOI: 10.1117/1.3116703]

Subject terms: ballistic chronograph; bullet; laser; uncertainty analysis; waveform analysis.

Paper 080332RR received May 1, 2008; revised manuscript received Jan. 30, 2009; accepted for publication Feb. 10, 2009; published online Apr. 20, 2009.

1 Introduction

Ballistic chronographs are used to measure the velocity of projectiles (bullets). This is important to help in developing formulas for different gunpowders and designing bullet shapes and gun components. For law enforcement and military applications, an even more important application is the assessment and characterization of ballistic armor ("bullet-proof" vests). Our purpose for developing this chronograph was to address ballistic armor assessment.

Ballistic armor is commonly evaluated using two types of tests: perforation testing, where bullets are fired at a specified velocity to verify that the armor will not be perforated, and V50 testing, where bullets are fired at different velocities to estimate the velocity above which half the shots would be expected to perforate the body armor and below which half the shots would not be expected to do so. (A shot is an event where one bullet is fired.) Reduced error and uncertainty in measuring the velocity of the bullet leads to greater confidence that velocities meet specifications and, for V50 testing, reduces the uncertainty in the estimated V50 value. Reproducibility between chronographs is also very important for interlaboratory comparisons of ballistic armor performance.

There have been several different technologies used for ballistic chronography. One popular type of ballistic chronograph uses radar technology, and another uses optical emitters with opposing optical detectors. The radar device is a conventional Doppler radar, where the bullet velocity is determined by the frequency shift of the reflected radio-frequency power from the approaching or receding bullet. The optical emitters with opposing optical detectors are often described as "light curtains" or "light screens;" they consist of a linear array of optical emitters lining a top bar and a linear array of optical detectors lining a bottom bar. The plane or other surface defined by the top bar and the bottom bar is usually perpendicular to the bullet trajectory. Two such light screens, separated by a known distance, are required. The bullet velocity is computed by dividing the distance between the two light screens by the time interval between the bullet blocking the light to an optical detector in the first, or *start*, light screen and blocking the light to an optical detector in the second, or *stop*, light screen. Since the bullet begins slowing down shortly after leaving the muzzle due to drag and other effects, the computed velocity is actually the average velocity of the bullet as it travels between the two light screens.

Other technologies that have been used include ultra-high-speed cameras and inductive sensors, essentially very high-speed metal detectors. The development of improved ballistic chronographs is an area of continued research, as evidenced by recent reports of two optical-based ballistic chronographs.[1,2]

The typical manufacturer-provided accuracy for the velocity estimate is ±1%. For a bullet velocity of 400 m/s (1312 ft/s), the ±1% accuracy corresponds to ±4 m/s (±13 ft/s). This accuracy may be adequate for characterization of ballistic armor, but since multiple chronographs give different measurement results, the performance of the chronographs must also be evaluated.

2 Measurement System

This measurement system was designed to provide an estimate of the projectile velocity with an associated uncertainty that is much lower than that of commercially available systems. This is accomplished by improving the determination of the instant that the bullet blocks the optical beam and providing an extensive uncertainty analysis of the measured velocity.

The ballistic chronograph comprises three components: the light source, the head, and the light detection component (Fig. 1). The chronograph head is mounted directly to the universal receiver or barrel of the firearm, using appropriate adapters (not shown). The light source and light detection components are located remote to the head and are connected to it using optical fiber cables of equal lengths.

The light source is a fiber-coupled cw semiconductor laser operating in the near IR (wavelength 1550 nm) with an optical output power that can easily saturate the response of all three optical detectors used in the light detection component. The single-mode, fiber-coupled output of the laser is split into three other fibers so that each fiber carries nominally equal power. Each of these fibers is then connected to a separate fiber pigtailed collimator that is mounted in the head. The collimators are FC-connectorized for easy takedown and assembly of the ballistic chrono-

0091-3286/2009/$25.00

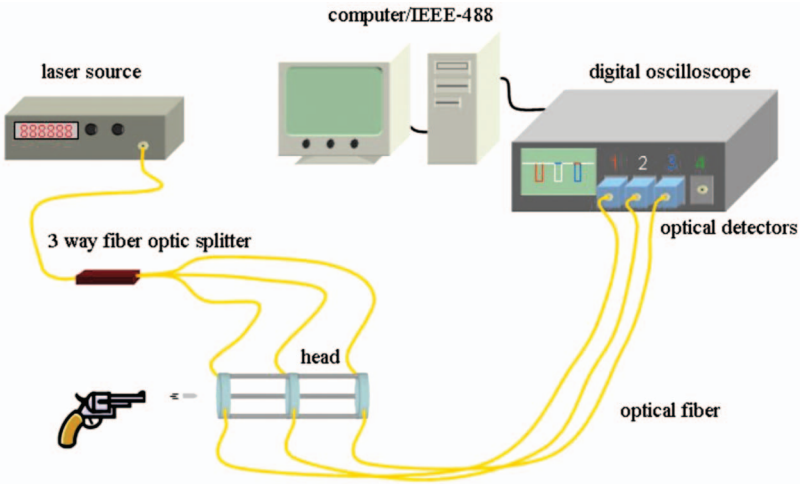

Fig. 1 Reference ballistic chronograph.

graph and for ease of repair. Several of the popular fiber optic connectors are mostly plastic. The metal ceramic construction of the FC connectors used here is assumed to add to the ruggedness of the system.

The chronograph head consists of several mechanical and optical components (Fig. 2). The optical components are the fiber pigtailed collimators already mentioned and collectors, arranged in pairs such that the output of the collimator faces the input of the collector with their optical axes nominally collinear. The commercially available collector is a small lens mounted in an FC connector. There are three collimator-collector pairs; each pair is mounted in a separate aluminum mounting flange, which establishes the spacing between each collimator and its associated collector. Each of these flanges is attached to the other using fixed-length, Invar®[*] posts. The spacing between beam centers of each pair in the assembled head is nominally 8 cm. The light detection component includes the light collectors, the optical detectors, and the waveform recorder (for which we use a real-time digital oscilloscope). The collectors and optical detectors are connected by 500-μm-core multimode fiber, which was selected to maximize light collection and minimize sensitivity to misalignment and shock. These fibers are connected to amplified indium gallium arsenide (InGaAs) photodiodes having a 3-dB attenuation bandwidth of 125 MHz and output impedance of 50 Ω. These three optical detectors are each connected to a different input channel of the oscilloscope. The oscilloscope has a 3-dB attenuation bandwidth of 350 MHz.

3 Operation

In operation, the bullet blocks each of the three laser beams in sequence, and in response the three amplified optical detectors each output a negative-going electrical pulse waveform. These three pulse waveforms are captured using three channels of the oscilloscope. The first electrical pulse is also used to trigger the oscilloscope. Along with the other two pulse waveforms created when the bullet blocked the other succeeding two laser beams, these waveforms are acquired and analyzed. The intervals between the three pulses, together with the knowledge of the physical spacing of the laser beams, are used to calculate the velocity of the bullet. Figure 3 depicts the waveforms acquired with the oscilloscope and transferred to a computer for analysis. Each waveform typically consists of 10^4 data points. The noise seen in the waveforms depicted in Fig. 3 results from the laser, the optical detectors, the amplifiers, and the oscilloscope input channels. This noise is a significant contributor to the uncertainty in the 50% transition instant.

The reference ballistic chronograph described herein may be used to measure the velocity of bullets that range in diameter from about 0.5 mm (the effective diameter of the laser beam) to about 20 mm (the gap between a fiber optic collimator and collector). These limits are design limits, not fundamental physical ones. The range of bullet velocities

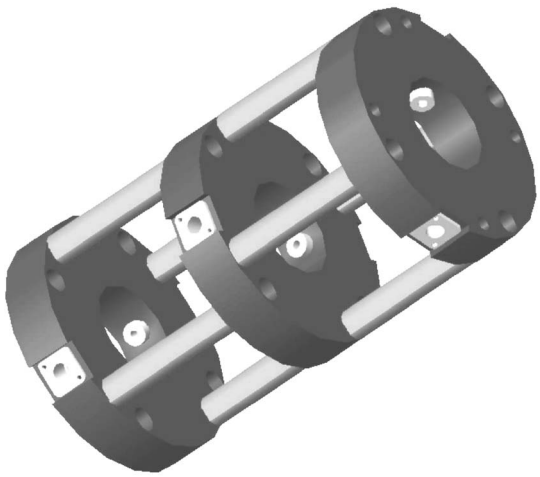

Fig. 2 Ballistic chronograph head without optical fibers.

[*] Certain commercial equipment, instruments, or materials are identified in this paper in order to specify the experimental procedure adequately. Such identification is not intended to imply recommendation or endorsement by the National Institute of Standards and Technology, nor is it intended to imply that the materials or equipment identified are necessarily the best available for the purpose.

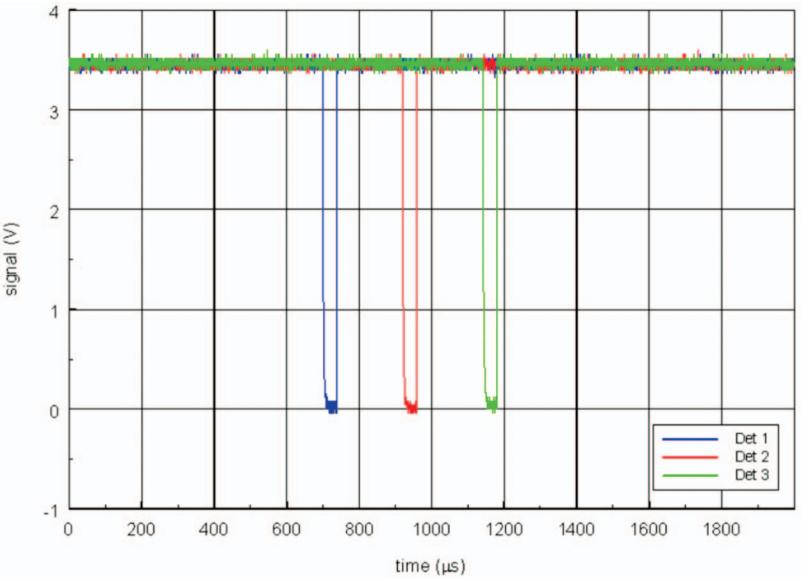

Fig. 3 Three waveforms acquired by oscilloscope.

that can be measured is set by a number of mechanical and electronic considerations and by the desired uncertainty. For the components used in the chronograph described herein and for the desired uncertainty (approximately 0.1% of bullet velocity), an estimate of the velocity range is 15 m/s to 10 km/s.

4 Measurement Results

The reference ballistic chronograph was tested using an ANSI/SAAMI test barrel mounted to a universal receiver.[3] Several different bullet shapes were used: .44-cal. magnum semi-wadcutters with a gas check, .357-cal. jacketed soft point, 9-mm hollow point, and 9-mm full metal jacket, round nose. Velocity estimates were compared with estimates from two or three commercially available ballistic chronographs. All three are optically based and similar to the reference ballistic chronograph; they sense the change in light level as the bullet passes between the light source and the optical detector.

Table 1 contains a few representative measurement results. B1 and B2 are two commercially available ballistic chronographs from the same manufacturer (same model) and their start and stop light screens are separated by 1 m. A1 is a commercially available ballistic chronograph from another manufacturer with the start and stop light screens separated by 0.345 m. The chronographs were arranged in a serial fashion; the reference ballistic chronograph was mounted at the end of the muzzle with the first optical beam located 0.29 m from the muzzle. Chronographs A1, B1, and B2 were located approximately 1.6, 2.0, and 2.1 m from the muzzle, respectively. However, the start light screens for B1 and B2 were immediately adjacent to each other, as were the stop light screens. This arrangement establishes a common bullet path through these two ballistic chronographs and minimizes differences in the measurement results due to drag. All testing occurred in the OLES Ballistics Range, an indoor facility located at the National Institute of Standards and Technology.

The data in Table 1 are not compensated for possible velocity variations of the bullet due to drag or other factors. It is provided to show the reader the possible magnitude of variation in measurement results from these instruments for a single shot.

5 Uncertainty Analysis

The bullet velocity is computed by dividing the distance traveled by the time it took for the bullet to travel that distance. The distance d is the separation between the axes of the laser beams from two adjacent collimator-collector pairs. The travel time t of the bullet is determined from the oscilloscope waveforms. The velocity s of the bullet is given in units of length (typically meters) per unit of time (seconds):

Table 1 Comparison of results.

	Velocity (m/s)			
Bullet	Reference ballistic chrono.	A1	B1	B2
9-mm round	444.0	444.1	440	440
9-mm round	408.7	408.5	406	406
9-mm hollow point	361.4	n/a	365	365
9-mm hollow point	382.2	n/a	383	380
0.357-cal.	535.9	535.8	531	531
0.44-cal. magnum	466.7	n/a	464	463

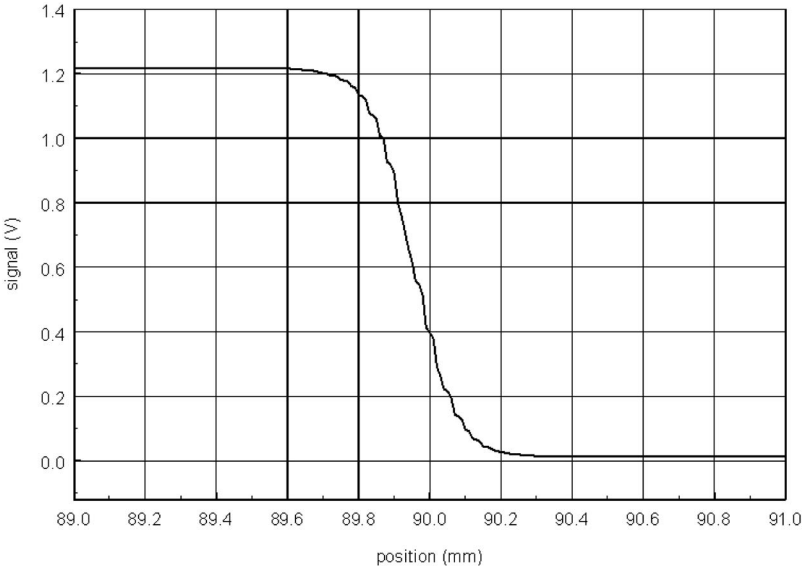

Fig. 4 Beam characterization waveform.

$$s = \frac{d}{t}. \tag{1}$$

The uncertainty u_s in the velocity estimate is

$$u_s = \left(\frac{u_d^2}{t^2} + \frac{u_t^2 d^2}{t^4} + u_r^2 \right)^{1/2}, \tag{2}$$

where u_d is the uncertainty in d, u_t is the uncertainty in t, and u_r is the variability in the velocity estimates. The contributors to the uncertainties u_d, u_t, and u_r are considered in the following subsections.

5.1 *Uncertainty u_d in Distance Traveled*

The contributions to the uncertainty u_d in the distance d are considered in the following sub-subsections. The distance between the optical beams is measured using a knife-edge attached to a stepping-motor-driven stage and a digital voltmeter connected to the optical detectors. The knife-edge is passed through each of the three optical beams in a path that is nominally collinear with that of the bullet. As the knife-edge passes through the optical beam, the laser energy coupled into the optical detector decreases and is eventually blocked completely. The output signal of the optical detector tracks this optical input, and it is this output signal that is monitored by the voltmeter. For each voltage reading acquired, V_i, the stage position x_i is also acquired, where i is the positional index, thus providing signal levels as a function of position. The set of these data pairs forms a step-like waveform (see, as an example, Fig. 4) that starts from a high state level, corresponding to the situation when the laser light is not blocked by the knife-edge, and then transitioning to a low state level, which corresponds to when the laser light is blocked from entering the optical detector.

The transition region contains information on the beam diameter at the location where the knife-edge passes through it. The beam diameter can be determined by taking the derivative of the steplike waveforms that were obtained when measuring the distance between collimator-collector pairs and then computing the e^{-2} points of the resultant Gaussian-like waveform. The collimation of the beams was checked by performing similar beam profile measurements near the collimator and also near the collector. The beams' diameters, measured near the center of the head, were nominally 500 μm, and the standard deviation of the beam diameter measurements was nominally ± 0.6 μm. When measured 4 mm on either side of the axis of the head, the nominal beam diameter changed less than 5 μm.

5.1.1 *Uncertainty in distance between optical beams*

Since there are three collimator-collector pairs, we obtain three $V(x_i)$ waveforms, one for each of the pairs. The distance $d_{2\text{-}1}$ between the laser beam propagating between the first collimator-collector pair and the laser beam propagating between second collimator-collector pairs is computed using

$$d_{2\text{-}1} = p_2 - p_1, \tag{3}$$

where p_1 and p_2 are the computed positions of the beam centers for the first and second collimator-collector pair, respectively. The beam center is the 50% reference level position of the steplike waveform. Since each of these data pair sets is acquired M times, we can compute the mean distance for $d_{2\text{-}1}$ (as an example) using

$$\bar{d}_{2\text{-}1} = \frac{1}{M} \sum_{m=1}^{M} d_{2\text{-}1,m}, \tag{4}$$

and its standard deviation $\sigma_{d,2\text{-}1}$ using

$$\sigma_{d,2\text{-}1} = \left\{ \frac{1}{M} \sum_{m=1}^{M} (\bar{d}_{2-1} - d_{2-1,m})^2 \right\}^{1/2}. \tag{5}$$

A similar computation is done for $d_{3\text{-}2}$ using p_2 and p_3.

5.1.2 *Uncertainty in beam position*

The distance between the laser beams is dependent on the estimate of the position of the laser beam centers, p_1, p_2, and p_3. As previously stated, p_1 is the value of the 50% reference level position of the first laser beam. Let u_{p_1} be the uncertainty in the position value for p_1 (which includes interpolation effects), u_{p_2} the uncertainty in the position value for p_2, u_{p_3} is the uncertainty in the position value for u_{p_3}, and u_{pos} the uncertainty in positioning of and/or in the reading of the position of the stepping motor translation stage. The multiplier 2 appears in front of u_{pos} in Eq. (6) because two separate positions are used to determine the distance. We have previously calculated the uncertainty[4] in determining reference level instants (see Ref. 5, IEEE Std. 181-2003, for description of terms), which are identical for computational purposes to the position values (p_i, $i=1,2,3$) described here. Using this analysis, we find the uncertainties, u_{p_1}, u_{p_2}, and u_{p_3} to each be ± 5 μm. The uncertainty, u_{pos}, in positioning the stepping motor stage, estimated from the manufacturer's specifications, is less than ± 0.5 μm.

5.1.3 *Uncertainty in distance estimate due to thermal expansion of the head*

The distance between laser beams is nominally 8 cm, of which 2 cm is contributed by the aluminum collimator-collector mounting flange, and 6 cm is contributed by the Invar® posts. Thermal expansion or contraction of these materials will cause changes in the distance between the laser beams. Although the temperature of the NIST Ballistics Range is well controlled, any temperature variations will result in small differences in velocity estimates. Assuming a difference in ambient temperature of 4 K between calibration of the distance between laser beams and a bullet velocity measurement, the uncertainty $u_{d(T)}$ in the laser beam separation for this head configuration is ± 2.2 μm. The use of Invar® posts helps minimize this variation.

5.1.4 *Combined uncertainty in the distance estimate*

The combined uncertainty in the distance between beam centers is computed using

$$u_{d,2\text{-}1} = (\sigma_{d,2\text{-}1}^2 + u_{p_1}^2 + u_{p_2}^2 + 2u_{\mathrm{pos}}^2 + u_{d(T)}^2)^{1/2}, \tag{6}$$

where the contributions to $u_{d,2\text{-}1}$ and their values are

$$\sigma_{d,2\text{-}1} = \pm 4.1\ \mu\mathrm{m},$$

$$u_{p_1} = \pm 5\ \mu\mathrm{m},$$

$$u_{p_2} = \pm 5\ \mu\mathrm{m},$$

$$u_{\mathrm{pos}} = \pm 0.5\ \mu\mathrm{m},$$

$$u_{d(T)} = \pm 2.2\ \mu\mathrm{m}.$$

The value of $u_{d,2\text{-}1}$ for typical measurement results and conditions, such as for the waveforms shown in Fig. 3, is ± 8.5 μm. The value of $u_{d,3\text{-}2}$ is the same.

5.2 *Uncertainty in the Time for the Distance Traveled, u_t*

The time corresponding to the distance traveled by the bullet is computed by taking the difference between the appropriate reference level instant of the waveforms acquired from each of the three channels to which an optical detector is attached. We select the 50% reference level instant because the estimate of the 50% reference level is less affected by noise than other reference levels. Noise is important with these waveforms because no averaging is performed (these are single-shot measurements). Before developing a mathematical expression that describes u_t, we first describe the factors that can contribute to the uncertainty in t.

5.2.1 *Chronograph-head-related factors contributing to u_t*

All nonideal mechanical and geometrical factors can contribute to u_t. These factors include the following:

1. Bullet trajectory is not coaxial with the axis of the head.
2. Bullet trajectory is changing (spiraling, wobbling, monotonic displacement with distance) as it passes through the head.
3. Bullet is not normal to the beams.
4. Optical beam profile is different amongst the beams.
5. Optical beams are not normal to the head axis.
6. Recoil changes the effective distance between successive collimator-collector pairs.

Although it is possible to derive mathematical expressions describing these contributions, it is not necessary. Information on these effects is contained, redundantly, in the acquired time-domain waveforms. For example, if the bullet, for whatever reason, does not present the same profile to each laser beam as it passes through the three beams, three effects will be observed: variation in the values of the first transition durations,[5] variation in the values of the second transition durations, and variation in the values of the pulse durations. Any one to all of the six reasons listed can cause this difference. The first transition corresponds to the nose of the bullet (which may be pointed or flat) and the second to the tail of the bullet (which is almost always nominally flat); the variation in the first transition duration values will be more sensitive to the mechanical and geometric factors than that for the second transition. However, in order to minimize the effects of blowby, the optical detectors are operated in saturation by increasing the optical power from the laser. Consequently, the duration of the first transition is significantly longer than that of the second transition. The pulse duration is also increased by operating the optical detectors in saturation. This masks some of the bullet shape and trajectory effects on the first transition duration and on the pulse duration. However, the variation in the second transition durations should still indicate these effects. Since

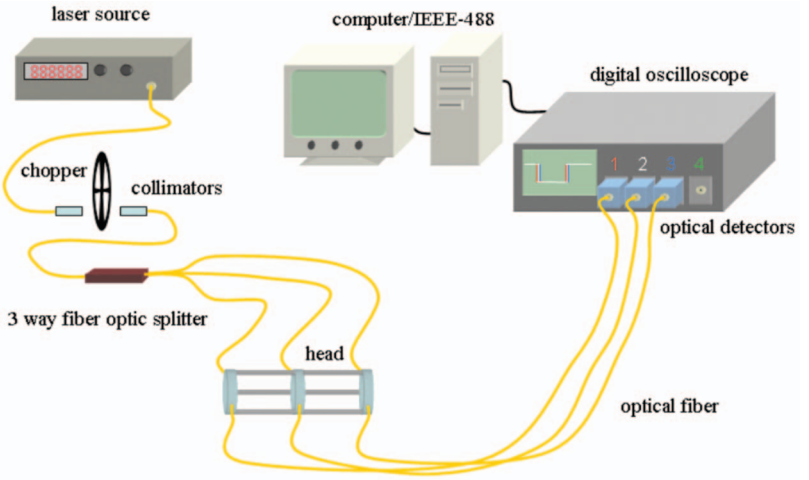

Fig. 5 Chronograph with chopper and fiber optic collimators.

the second transition duration is also the shortest, it is used to calculate the velocity and u_t. We can calculate the mean of these transition durations using

$$\bar{\tau}_i = \frac{1}{N}\sum_{n=1}^{N} \tau_{i,n}, \tag{7}$$

where $\tau_{i,n}$ is the transition duration of the waveform taken from each of the three channels of the oscilloscope, i is the transition index ($i=1$ being the first, or negative, transition, and $i=2$ the second, or positive, transition), and the subscript n denotes one of the three oscilloscope channels, which corresponds to one of the collimator-collector pairs, and $N=3$. The standard deviation for the mean transition duration values is

$$\sigma_{\tau_i} = \left[\frac{1}{N}\sum_{n=1}^{N} (\bar{\tau}_i - \tau_{i,n})^2\right]^{1/2}. \tag{8}$$

We have previously developed an analysis to determine the uncertainty in transition duration values[4] that includes the standard deviation, instrument effects, computational effects, sampling interval size, etc. However, the uncertainties due to these other effects are small compared to the standard deviation in the transition duration values and so can be ignored.

5.2.2 *Timebase calibration*

The oscilloscope timebase must be calibrated to ensure the sampling interval is known and uniform. If not, these errors may have to be corrected and/or appropriate uncertainties attributed to the temporal information of the waveforms. The timebase error, $u_{\Delta t}$, was measured using known sine-wave signals in a method described in Ref. 6. The linear part of the timebase error can be easily corrected by correcting the value of the sampling interval. The variation between the linear fit to the timebase values and the actual measured values is used to compute $u_{\Delta t}$. For the oscilloscope used in this study, $u_{\Delta t}$ was determined to be ± 0.7 ns.

5.2.3 *Different delays between chronograph head and initial instants of waveforms*

This delay has three primary sources: different lengths of fiber optic cable running between the chronograph head and the optical detector, different operating delays of the optical detectors, and skew between channels of the oscilloscope. Because the optical pulses generated have a transition duration of about 0.4 μs or more, any pulse distortion resulting from modal dispersion would be very small and very similar for each signal path. It is neglected here. Differences in optical fiber cable lengths as much as ± 0.5 m will introduce time delay differences of about ± 2.5 ns, assuming a nominal propagation velocity of 2×10^8 m/s. This and the other contributions can be measured simultaneously using the measurement setup in Fig. 5. A mechanical light chopper is inserted before the three-way optical fiber splitter and provides three almost simultaneously generated and nearly identical optical pulses to each of the three collectors and the corresponding optical detector and oscilloscope channels. We measured a differential delay of ± 10 ns from the three oscilloscope channels. Although this value includes differences in signal path from the laser to the collimators, differences that would not affect the measurement of bullet velocity, it is used as an estimate of u_Δ, the uncertainty due to differential delays.

5.2.4 *Combined uncertainty in the time estimate*

The uncertainty in the time estimate for the distance traveled is given by

$$u_t = (\sigma_{\tau_2}^2 + u_{\Delta t}^2 + u_\Delta^2)^{1/2}, \tag{9}$$

where σ_{τ_2} is the uncertainty in the second transition durations of the pulses, $u_{\Delta t}$ is the uncertainty in the oscilloscope timebase, and u_Δ is the uncertainty due to the differential delay. Typical values for the contributors to u_t

are

$$\sigma_{\tau_2} = \pm 24.6 \text{ ns},$$

$$u_{\Delta t} = \pm 0.7 \text{ ns},$$

$$u_{\Delta} = \pm 10 \text{ ns}.$$

The value of u_t for typical measurement results and conditions, such as for the waveforms shown in Fig. 3, is 26.6 ns.

5.3 *Velocity Uncertainty u_s*

The velocity is determined using a linear least-squares fit to the three distance-time data points. The velocity is the reciprocal of the slope of the fitted line. The uncertainty u_r due to the variability of this velocity determination is found using the standard error of the slope and is given by

$$u_r = [u_e^2(y)/y^4]^{1/2}, \tag{10}$$

where u_e is the standard error of the slope y. A typical value for u_r is 0.07 m/s.

The preceding uncertainty estimates for distance, time, and velocity are combined using the root-sum-of-squares method shown in Eq. (2) and reproduced as follows:

$$u_s = \left(\frac{u_d^2}{t^2} + \frac{u_t^2 d^2}{t^4} + u_r^2 \right)^{1/2}.$$

The effective degrees of freedom are estimated using the Welch-Satterthwaite formula, and the coverage factor is found from the t-distribution for a 95% level of confidence.[7] The expanded uncertainty is the product of the coverage factor (2.0 for 95% confidence) and the combined uncertainty.[7] For the waveforms shown in Fig. 3 and the measurement conditions, we get $s = 361.4 \pm 0.2$ m/s. The expanded uncertainty is about 0.05% of the velocity, compared to about 1% for commercial ballistic chronographs.

6 Conclusion

By using a waveform recorder (oscilloscope) and pulse analysis techniques, a ballistic chronograph can be developed that provides velocity estimates with at least an order of magnitude lower uncertainty than commercially available ballistic chronographs. Because of this low uncertainty, this chronograph can be used as a reference to calibrate and/or characterize the performance of commercially available chronographs.

Acknowledgments

We would like to thank Nathaniel Waters for providing access to and running the firing range and to Kirk Rice for providing information on performance requirements and editorial assistance. We also acknowledge William Guthrie's assistance with the uncertainty analysis.

References

1. R. C. Kalonia et al., "Laser-based projectile speed measurement system," *Opt. Eng.* **46**(4), 044303-1–6 (2007).
2. J. M. Sánchez-Pena, C. Marcos, M. Y. Fernández, and R. Zaera, "Cost-effective optoelectronic system to measure the projectile velocity in high-velocity impact testing of aircraft and spacecraft structural elements," *Opt. Eng.* **46**(5), 051014-1–6 (2007).
3. ANSI/SAAMI Z299.3-1993, "Voluntary industry standards for pressure and velocity of centerfire pistol and revolver ammunition for the use of commercial manufacturers," Sporting Arms and Ammunition Manufacturers' Inst., Newtown, CT (1993).
4. N. G. Paulter and D. R. Larson, "Pulse parameter uncertainty analysis," *Metrologia* **39**(2), 143–155 (2002).
5. IEEE Std. 181-2003, "Standard on transitions, pulses, and related waveforms," Inst. of Electrical and Electronic Engineers, Piscataway, NJ (2003).
6. G. N. Stenbakken and J. P. Deyst, "Time-base nonlinearity determination using iterated sine-fit analysis," *IEEE Trans. Instrum. Meas.* **47**(5), 1056–1061 (1998).
7. *ISO Guide to the Expression of Uncertainty in Measurement*, ISO, Geneva (1993).

Nicholas G. Paulter, Jr., received the MS degree in chemistry from the University of New Mexico, Albuquerque, in 1988 and the MS degree in electrical engineering from the University of Colorado, Boulder, in 1990. He was with Los Alamos National Laboratory, Los Alamos, NM, from 1980 to 1989, and was involved in the study of fast electrical phenomena and in the development of high-speed photoconductors for use as ultrafast light detectors and sampling gates. In 1989, he joined the National Institute of Standards and Technology (NIST), Boulder, to develop transient pulse measurement techniques and analysis. He is currently a program manager with the Office of Law Enforcement Standards at NIST in Gaithersburg, MD. His present research interests include semiconductor physics, materials properties, electro-optics, ultrafast electronic phenomena, and waveform and data processing and analysis.

Donald R. Larson received a BS degree (cum laude) from Brigham Young University (1978) and a MSEE degree from the University of Colorado in Boulder (1981). He worked at the National Institute of Standards and Technology (NIST) in Boulder, Colorado, from 1976 until 1998 in the Optoelectronics Division. Since 1998, he has been at NIST in Gaithersburg, MD, first in the Quantum Electrical Metrology Division (formerly known as the Electricity Division) and now in the Office of Law Enforcement Standards.